

A meson-exchange model of the associated photoproduction of vector mesons and $N^*(1440)$ resonances

Madeleine Soyeur

*Département d'Astrophysique, de Physique des Particules,
de Physique Nucléaire et de l'Instrumentation Associée,
Service de Physique Nucléaire,
Commissariat à l'Energie Atomique/Saclay,
F-91191 Gif-sur-Yvette Cedex, France*

We discuss the photoproduction of ω - and ρ^0 -mesons off protons in the particular channel where the target proton is excited to a Roper resonance $N^*(1440)$. We propose a simple meson-exchange model for these processes in order to evaluate their cross sections near threshold and at low momentum transfers. It is suggested in particular that the differential cross section for the associate photoproduction of a ρ^0 -meson and a Roper resonance in these kinematic conditions could provide direct information on the strength of the scalar-isoscalar excitation of the $N^*(1440)$ and hence on the magnitude of an effective $\sigma NN^*(1440)$ coupling. The latter quantity is poorly known and of much interest for the nuclear many-body problem.

PACS: 13.60.Le, 13.60.Rj, 14.20.Gk

Keywords: Vector meson photoproduction, Roper resonance

1 Introduction

The Roper resonance, the $N_{1/2,1/2}^*(1440)$, is the first excited state of the nucleon. It is a broad state, with an estimated full width of 350 MeV, which couples strongly (60-70 %) to the π -nucleon channel and significantly (5-10 %) to the σ -nucleon (more properly $(\pi\pi)_{S=0}^{I=0}$ -nucleon) channel [1].

The low excitation energy and the particular decay scheme of the Roper resonance suggest that it could play an important role in nuclear dynamics as virtual intermediate state. For example, a repulsive three-nucleon interaction can be generated by the π - and σ -exchange components of the nucleon-nucleon

interaction with an intermediate $N^*(1440)$ [2]. The corresponding graph is displayed in Fig. 1. The importance of the three-nucleon interaction generated by

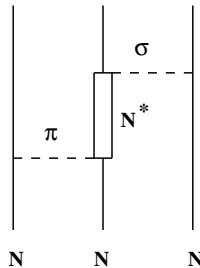


Fig. 1. $\pi\sigma$ -exchange three-nucleon interaction involving the excitation of the $N^*(1440)$ resonance.

this process depends on the $\pi NN^*(1440)$ and $\sigma NN^*(1440)$ coupling strengths. The uncertainty in the total width of the $N^*(1440)$ and in its branching ratio to the πN channel implies that the πNN^* coupling constant is known with an accuracy of about 50%. The indetermination in the effective σNN^* coupling constant is much larger, typically a factor of 2-3. Consequently, the magnitude of the matrix element of the three-nucleon interaction of Fig. 1 in the triton groundstate for example will be quite uncertain. With a rather low value of the σNN^* coupling constant, it has been shown in Ref. [2] that the repulsive three-nucleon contribution to the triton binding energy corresponding to the diagram of Fig. 1 gets largely cancelled by the attractive contribution of a similar diagram, in which the σ -exchange is replaced by the ω -exchange. Were the σNN^* coupling constant much larger, this cancellation would not occur, leading to a possibly significant repulsive three-body contribution to the triton binding energy. Such contribution would also influence the properties of the four-nucleon system [3].

The $\pi NN^*(1440)$ and $\sigma NN^*(1440)$ coupling strengths play also a role in the dynamics of neutral pion production in proton-proton collisions near threshold [4]. In $pp \rightarrow pp\pi^0$, π^0 production on a single proton underestimates largely the cross section and the main π -exchange term is suppressed by the particular isospin structure of the reaction [5]. The $pp \rightarrow pp\pi^0$ cross section is therefore directly related to short-range exchanges. The contribution from virtual intermediate $N^*(1440)$ resonances is sizeable and enhances the cross section, unlike the contributions from the neighbouring $N^*(1535)$ and $N^*(1520)$ resonances which decrease it [4]. The graph of Fig. 2 is the main term involving the excitation of the $N^*(1440)$ resonance and again depends sensitively on the $\pi NN^*(1440)$ and $\sigma NN^*(1440)$ couplings.

The strong coupling of the $N^*(1440)$ to the πN and σN channels could also be of importance for the evolution of nonequilibrium nuclear systems. In heavy ion collisions at relativistic energies ($E/A \simeq 1-2$ GeV), baryon resonances are excited during the initial stage of the reaction, when the colliding nuclei

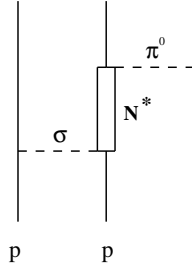


Fig. 2. σ -exchange contribution to the $pp \rightarrow pp\pi^0$ cross section involving the excitation of the $N^*(1440)$ resonance.

form a very dense nuclear system [6,7]. In later stages, their interactions and decays influence strongly the production of hadrons [8,9]. It is particularly so for the production of subthreshold particles because the internal energy stored in intrinsic baryonic excitations increases the two-body phase space of the subsequent collisions and helps in making higher mass hadrons [9]. In this perspective, the excitation of the $N^*(1440)$ appears to play a major role in explaining the production of antiprotons in heavy ion collisions at subthreshold energies ($E/A = 2$ GeV) [9].

To describe relativistic heavy ion collisions starting from an effective Lagrangian of interacting baryons and mesons, the relevant meson-baryon couplings have to be determined. The standard procedure is to fix these couplings using measured decay rates and simple scattering processes in free space. For the specific investigation of the behaviour of the Roper resonance in relativistic heavy ion collisions, the relevant parameters were computed from the known partial decay rates of the $N^*(1440)$ and by describing the available data on the $pp \rightarrow pN^*(1440)$ cross section using a one-boson exchange model [10,11]. The $\pi NN^*(1440)$ and $\sigma NN^*(1440)$ coupling strengths are important inputs in such model. Coupled relativistic transport equations of the Boltzmann-Uehling-Uhlenbeck type for nucleons, $\Delta(1232)$ and $N^*(1440)$ resonances have then been derived and solved to study consistently the mean fields and the in-medium two-body scattering cross sections of these baryons [11].

The need for a proper account of the effects of the $N^*(1440)$ in the description of relativistic heavy ion collisions is particularly motivated by a recent result of the FOPI Collaboration at GSI [12]. The comparison of (p, π^+) and (p, π^-) pair cross sections in Ni+Ni reactions indicates the presence of $I=1/2$ resonance contributions with a mean free mass above the $\Delta(1232)$ mass. This contribution is of the order of 20 % [12]. The low-energy tail of the $N^*(1440)$ seems a natural explanation of this effect.

From the above discussion, it appears of much interest to single out processes where the excitation of the Roper resonance by the π -field, and even more importantly, by the σ -field dominates the dynamics. We suggest that the photoproduction of ω - and ρ -mesons off protons in association with the exci-

tation of the target to a $N^*(1440)$ resonance, the $\gamma p \rightarrow \omega N^{*+}(1440)$ and the $\gamma p \rightarrow \rho^0 N^{*+}(1440)$ reactions, studied in the proper kinematics (near threshold and at low q^2) could be such processes.

Section 2 is devoted to a discussion of the $\pi NN^*(1440)$ and $\sigma NN^*(1440)$ couplings. Using a simple meson-exchange picture, the relation between these couplings and the $\gamma p \rightarrow \omega N^{*+}(1440)$ and the $\gamma p \rightarrow \rho^0 N^{*+}(1440)$ reaction cross sections near threshold is exhibited in Section 3. The calculated differential cross sections for the $\gamma p \rightarrow \omega N^{*+}(1440)$ and the $\gamma p \rightarrow \rho^0 N^{*+}(1440)$ processes and their dependence on the strength of the excitation of the Roper resonance by the π - and σ -fields are presented in Section 4. We conclude by a few remarks in Section 5.

2 The $\pi NN^*(1440)$ and $\sigma NN^*(1440)$ couplings

2.1 The $\pi NN^*(1440)$ coupling

The $\pi NN^*(1440)$ coupling constant can be calculated from the partial decay width of the Roper resonance to the πN channel [1]. We assume the pseudoscalar πNN^* coupling Lagrangian,

$$\mathcal{L}_{\pi NN^*}^{int} = -ig_{\pi NN^*} \bar{N}^* \gamma_5 (\vec{\tau} \cdot \vec{\pi}) N + h.c., \quad (1)$$

where $g_{\pi NN^*}$ is the $\pi NN^*(1440)$ coupling constant. It is related to the partial decay width of the $N^*(1440)$ into the πN channel by

$$\Gamma_{N^* \rightarrow \pi N} = 3 \frac{g_{\pi NN^*}^2}{4\pi} \frac{E - M_N}{M_{N^*}^0} p(E), \quad (2)$$

where $M_{N^*}^0$ is the Breit-Wigner mass of the Roper resonance, E the nucleon energy in the rest frame of the decaying $N^*(1440)$ at the peak of the resonance,

$$E = \frac{M_{N^*}^{02} + M_N^2 - m_\pi^2}{2M_{N^*}^0}, \quad (3)$$

and $p(E)$ is the corresponding nucleon momentum. To compare to other derivations, it is useful to note the relation between $g_{\pi NN^*}$ and $f_{\pi NN^*}$,

$$\frac{g_{\pi NN^*}^2}{4\pi} = \frac{f_{\pi NN^*}^2}{4\pi} \frac{(M_{N^*}^0 + M_N)^2}{m_\pi^2}, \quad (4)$$

in which $f_{\pi NN^*}$ is the coupling constant for the pseudovector πNN^* interaction Lagrangian,

$$\mathcal{L}_{\pi NN^*}^{int} = -\frac{f_{\pi NN^*}}{m_\pi} \bar{N}^* \gamma_5 \gamma_\mu \partial^\mu (\vec{\tau} \cdot \vec{\pi}) N + h.c.. \quad (5)$$

Assuming that the branching ratio of the $N^*(1440)$ resonance into the πN channel is 60-70 % of the total width (350 ± 100) MeV [1], the partial decay width $\Gamma_{N^* \rightarrow N\pi}$ is 228 MeV with an error bar of 82 MeV. Inserting these numbers in Eq. (2), we get

$$\frac{g_{\pi NN^*}^2}{4\pi} = 3.4 \pm 1.2. \quad (6)$$

The value of $g_{\pi NN^*}^2/4\pi$ obtained in Ref. [10] is 1.79. The value of $f_{\pi NN^*}^2/4\pi$ corresponding to Eq. (6) is (0.011 ± 0.004) , to be compared to 0.031 used in Ref. [2], 0.018 in Ref. [13] and 0.008 in Ref. [14]. The coupling constant of Ref. [13] is obtained using the nonrelativistic limit of Eq. (5).

2.2 The $\sigma NN^*(1440)$ coupling

We describe the $\sigma NN^*(1440)$ coupling by the interaction Lagrangian,

$$\mathcal{L}_{\sigma NN^*}^{int} = -g_{\sigma NN^*} \bar{N}^* \sigma N + h.c.. \quad (7)$$

The relation between the $\sigma NN^*(1440)$ coupling constant and the partial decay width of the Roper resonance into the $(\pi\pi)_{S=0}^{I=0}$ -nucleon channel is model-dependent. We assume that it can be described by the process displayed in

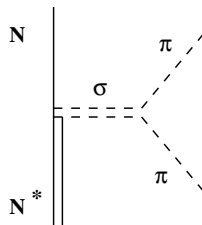


Fig. 3. Roper resonance decay into the $(\pi\pi)_{S=0}^{I=0}$ -nucleon channel through an intermediate σ -meson.

Fig. 3. In this process, the $\sigma\pi\pi$ coupling is taken to be of the form

$$\mathcal{L}_{\sigma\pi\pi}^{int} = \frac{1}{2} g_{\sigma\pi\pi} m_\sigma^0 \bar{\pi} \cdot \bar{\pi} \sigma, \quad (8)$$

where m_σ^0 is the σ -meson mass. The link between the coupling constant $g_{\sigma NN^*}$ and the $N^*(1440) \rightarrow N(\pi\pi)_{S-wave}^{I=0}$ decay rate depends on the mass and width of the intermediate σ -meson. The σ -meson under consideration in vector meson photoproduction (to be discussed in Section 3) is the effective degree of freedom accounting for the exchange of two uncorrelated as well as two resonating pions [15]. Its mass is of the order of 500 MeV and it should be a broad object. The phase space available for the two-pion invariant mass ranges from $2m_\pi$ until $M_{N^*}^0 - M_N$, the latter mass difference being of the order of 500 MeV. The mass of the effective σ -meson is therefore very close to the edge of phase-space for the $N^*(1440) \rightarrow N\pi\pi$ decay.

Using Eqs. (7) and (8), the partial width for the $N^*(1440)$ decay into the $N(\pi\pi)_{S-wave}^{I=0}$ channel in the intermediate σ model depicted in Fig. 3 is

$$\Gamma_{N^* \rightarrow N(\pi\pi)_{S-wave}^{I=0}} = \frac{g_{\sigma NN^*}^2}{4\pi} \int_{2m_\pi}^{M_{N^*}^0 - M_N} dm_\sigma \frac{(M_{N^*}^0 + M_N)^2 - m_\sigma^2}{2M_{N^*}^{02}} p(m_\sigma) W(m_\sigma), \quad (9)$$

in which the nucleon 3-momentum p and the σ spectral function W read

$$p(m_\sigma) = \frac{[M_{N^*}^{02} - (M_N + m_\sigma)^2]^{1/2} [M_{N^*}^{02} - (M_N - m_\sigma)^2]^{1/2}}{2M_{N^*}^0} \quad (10)$$

and

$$W(m_\sigma) = \frac{2\pi^{-1} m_\sigma m_\sigma^0 \Gamma_{\sigma \rightarrow \pi\pi}(m_\sigma)}{(m_\sigma^{02} - m_\sigma^2)^2 + m_\sigma^{02} \Gamma_{\sigma \rightarrow \pi\pi}^2(m_\sigma)}. \quad (11)$$

The energy-dependent width of the effective σ -meson is zero for $m_\sigma^2 < 4m_\pi^2$ and given by

$$\Gamma_{\sigma \rightarrow \pi\pi}(m_\sigma) = \Gamma_{\sigma \rightarrow \pi\pi}(m_\sigma^0) \left[\frac{m_\sigma^2 - 4m_\pi^2}{m_\sigma^{02} - 4m_\pi^2} \right]^{1/2} \quad (12)$$

for $m_\sigma^2 > 4m_\pi^2$. $\Gamma_{\sigma \rightarrow \pi\pi}(m_\sigma^0)$ denotes the width of the σ -meson at the peak of the resonance (m_σ^0). The parameters are m_σ^0 and $\Gamma_{\sigma \rightarrow \pi\pi}(m_\sigma^0)$. We fix m_σ^0 to be 500 MeV. We assume, quite arbitrarily, that the σ -meson has a width of 250 MeV, as the available data [1] do not allow its determination from the $\pi\pi$ phase shifts. Evaluating the integral of Eq. (9) with these values of the parameters, we find

$$\Gamma_{N^* \rightarrow N(\pi\pi)_{S-wave}^{I=0}} [MeV] = 75.8 \frac{g_{\sigma NN^*}^2}{4\pi} [MeV]. \quad (13)$$

The branching ratio of the $N^*(1440)$ into the $N(\pi\pi)_{S-wave}^{I=0}$ channel is 5-10 % of the total width of (350 ± 100) MeV [1]. The partial decay width $\Gamma_{N^* \rightarrow N(\pi\pi)_{S-wave}^{I=0}}$ is therefore (26 ± 16) MeV and Eq. (13) gives

$$\frac{g_{\sigma NN^*}^2}{4\pi} = 0.34 \pm 0.21. \quad (14)$$

It is important to study the sensitivity of this value to both m_σ^0 and $\Gamma_{\sigma \rightarrow \pi\pi}(m_\sigma^0)$. We have first varied $\Gamma_{\sigma \rightarrow \pi\pi}(m_\sigma^0)$ keeping $m_\sigma^0=500$ MeV fixed. We find that the value of $g_{\sigma NN^*}^2/4\pi$ increases slowly with $\Gamma_{\sigma \rightarrow \pi\pi}(m_\sigma^0)$. When $\Gamma_{\sigma \rightarrow \pi\pi}(m_\sigma^0)$ varies from 200 to 300 MeV, $g_{\sigma NN^*}^2/4\pi$ increases by about 6%. The sensitivity of $g_{\sigma NN^*}^2/4\pi$ to $\Gamma_{\sigma \rightarrow \pi\pi}(m_\sigma^0)$ is therefore rather low. In contrast to this behaviour, the value of $g_{\sigma NN^*}^2/4\pi$ depends strongly on m_σ^0 , because of the phase space limit mentioned above. Values of m_σ^0 lower than 500 MeV will lead to a relative increase of the integral in Eq. (9) while larger masses (such that m_σ^0 exceeds $M_{N^*}^0 - M_N$) will reduce it. Fixing $\Gamma_{\sigma \rightarrow \pi\pi}(m_\sigma^0)=250$ MeV, we find that Eq. (14) becomes

$$\frac{g_{\sigma NN^*}^2}{4\pi} = 0.23 \pm 0.14 \quad (15)$$

for $m_\sigma^0=450$ MeV and

$$\frac{g_{\sigma NN^*}^2}{4\pi} = 0.56 \pm 0.35 \quad (16)$$

for $m_\sigma^0=550$ MeV. Small variations in the σ -meson mass around 500 MeV reflect strongly in the value of $g_{\sigma NN^*}^2/4\pi$.

In Refs. [2,4], the effective σ -meson has no width and a mass m_σ^0 of 410 MeV. Assuming the experimental partial decay width $\Gamma_{N^* \rightarrow N(\pi\pi)_{S-wave}^{I=0}}$ to be 35 MeV, the authors get $g_{\sigma NN^*}^2/4\pi=0.1$ [2,4]. The mass-dependence mentioned above is largely responsible for this small coupling constant. The scaling relation for the meson- NN^* and meson- NN coupling constants used in Refs. [10,11] yields $g_{\sigma NN^*}^2/4\pi=0.05$. An effective value for $g_{\sigma NN^*}$ has been derived recently from data [16] on the excitation of the Roper resonance in the inelastic scattering of α particles off proton targets [17]. The reaction $\alpha + p \rightarrow \alpha + X$ is studied for incident α particles of 4.2 GeV. Missing energy spectra are measured at small angles (0.8, 2.0, 3.2 and 4.1°) [16]. The dominant inelastic processes contributing to the reaction are found to be the excitation of the Δ resonance in the projectile (followed by the emission of a pion) and the excitation of the Roper resonance in the target. The latter process is described by the exchange of a σ -meson between the incident α particle and the proton target [17]. In

order to reproduce the missing energy spectrum at 0.8° , the $\sigma NN^*(1440)$ coupling constant has to be quite large. The value corresponding to the best fit is $g_{\sigma NN^*}^2/4\pi = 1.33$ with a form factor $F_{\sigma NN^*} = (\Lambda_\sigma^2 - m_\sigma^2)/(\Lambda_\sigma^2 - q^2)$, where $\Lambda_\sigma = 1.7$ GeV and $m_\sigma^0 = 550$ MeV [17]. Clearly, the $\sigma NN^*(1440)$ coupling needed in this case appears stronger than inferred from the partial decay width of the $N^*(1440)$ in the $N(\pi\pi)_{S=0}^{I=0}$ channel. As remarked by the authors of Ref. [17], their σ -exchange interaction could simulate other exchanges of isoscalar character. It could also be that the strength observed in the missing energy spectrum around the position of the Roper resonance, after subtraction of the Δ background, should not be attributed entirely to the $N^*(1440)$. The analysis of more exclusive experiments is in progress. Preliminary data on the $p(d,d')N^*$ reaction at incident deuteron energies of 2.3 GeV, where the excitation of the $\Delta(1232)$ and of the $N^*(1440)$ are separated by the detection of the decay proton, seem to indicate that the excitation of the Roper resonance predicted using the parameters of Ref. [17] is larger than the observed cross-section [18], typically by a factor of two. If this effect could be confirmed, it would suggest that the analysis of the $p(d,d')N^*$ reaction leads to an effective value of $g_{\sigma NN^*}$ quite close to the phenomenological coupling constant given in Eq. (16) for $m_\sigma^0 = 550$ MeV.

The coupling constants of the $N^*(1440)$ to meson-nucleon channels determined from partial decay widths in this Section will be used later to describe vertices in t-channel meson-exchange processes. That these couplings are taken to be identical in both channels is in general an approximation. It is particularly so in the case of the effective σ -meson exchange which involves explicitly the resummation of many processes.

3 Meson-exchange model for the $\gamma p \rightarrow \omega N^{*+}(1440)$ and the $\gamma p \rightarrow \rho^0 N^{*+}(1440)$ reactions near threshold

The presently available data [19] on the photoproduction of ω - and ρ^0 -mesons off proton targets near threshold ($E_\gamma \leq 2$ GeV) can be described at low momentum transfers ($|q^2| \leq 0.5\text{-}0.6$ GeV²) by a simple one-meson exchange model [15]. Charge conjugation invariance forbids the exchange of vector mesons in this approximation. The cross section for the $\gamma p \rightarrow \omega p$ and $\gamma p \rightarrow \rho^0 p$ reactions are therefore obtained by summing π - and σ -exchange contributions. Moreover the π - and σ -exchanges play a very different role in the photoproduction of ω - and ρ^0 -mesons. The $\gamma p \rightarrow \omega p$ cross section can be understood as given entirely by π -exchange while the $\gamma p \rightarrow \rho^0 p$ reaction is dominated by σ -exchange [15]. At higher energies, typically for $E_\gamma > 2.5$ GeV (i.e. ~ 1.5 GeV above threshold), this simple meson-exchange model does no longer describe the data and the cross sections develop a large diffractive component.

The Roper resonance being the lowest excited state of the nucleon, with similar quantum numbers, it is tempting to use the meson-exchange model of Ref. [15] to describe the $\gamma p \rightarrow \omega N^{*+}(1440)$ and $\gamma p \rightarrow \rho^0 N^{*+}(1440)$ reactions close to threshold and at low q^2 . The cross sections for these processes in the limited kinematic regime mentioned above could be good experimental measures of the strength of the $\pi N N^*(1440)$ and $\sigma N N^*(1440)$ couplings.

The one-boson exchange contributions to the $\gamma p \rightarrow \omega N^{*+}(1440)$ and $\gamma p \rightarrow \rho^0 N^{*+}(1440)$ reactions in the Vector Dominance Model [20] are shown in Figs. 4 and 5 respectively.

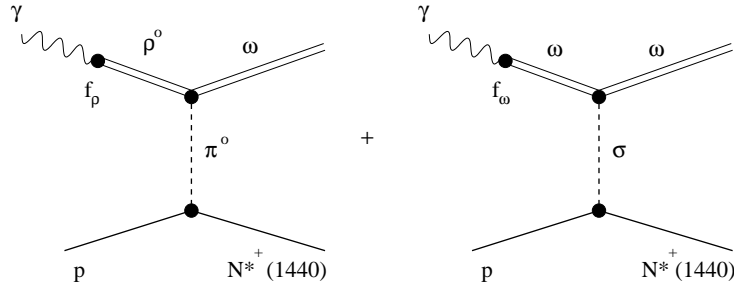


Fig. 4. Diagrams contributing to the $\gamma p \rightarrow \omega N^{*+}(1440)$ cross section in the one-boson exchange model.

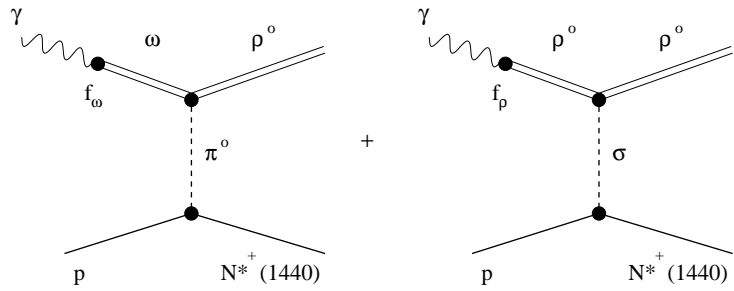


Fig. 5. Diagrams contributing to the $\gamma p \rightarrow \rho^0 N^{*+}(1440)$ cross section in the one-boson exchange model.

3.1 The $\gamma p \rightarrow \omega N^{*+}(1440)$ reaction

We consider first the $\gamma p \rightarrow \omega N^{*+}(1440)$ process ($E_\gamma^{threshold} = 2.16$ GeV at the peak of the Roper Resonance) and follow closely the discussion of Ref. [15].

We expect the σ -exchange diagram to be completely negligible compared to the π -exchange diagram. From the experimental data [1] on the partial decay widths $\omega \rightarrow \pi^0 \gamma$ $[(0.72 \pm 0.04) \text{ MeV}]$ and $\omega \rightarrow \pi^0 \pi^0 \gamma$ $[(0.61 \pm 0.21) \text{ keV}]$, it is easy to show, using the effective $\omega\pi\gamma$ and $\omega\sigma\gamma$ interaction Lagrangians of Ref. [21], that the coupling constant $g_{\omega\pi\gamma}^2/4\pi$ is about 100 times larger than $g_{\omega\sigma\gamma}^2/4\pi$. As discussed in Section 2, the $\pi NN^*(1440)$ coupling is also expected to be larger than the $\sigma NN^*(1440)$ coupling ($g_{\pi NN^*}^2/4\pi \simeq 2\text{-}5$ while $g_{\sigma NN^*}^2/4\pi \simeq 0.1\text{-}1.0$). We calculate therefore the differential cross section $d\sigma/dq^2$ for the $\gamma p \rightarrow \omega N^{*+}(1440)$ reaction assuming π -exchange only.

We describe the $\omega\pi\gamma$ coupling as in Ref. [15]. For completeness, we recall that we used in this work the ρ -dominance model of the vertex and the effective $\omega\rho\pi$ Lagrangian,

$$\mathcal{L}_{\omega\pi^0\rho^0}^{int} = \frac{g_{\omega\pi\rho}}{m_\omega} \varepsilon_{\alpha\beta\gamma\delta} \partial^\alpha \rho^{0\beta} \partial^\delta \omega^\rho \pi^0, \quad (17)$$

with $g_{\omega\pi\rho}^2/4\pi=6.7$. The non-locality of the $\omega\pi\rho$ vertex is fixed from the study of the $\omega \rightarrow \pi^0 \mu^+ \mu^-$ decay and given by the form factor $F_{\omega\pi\rho} = (m_\rho^2 - m_\pi^2)/(m_\rho^2 - q^2)$. We use for the $\pi NN^*(1440)$ vertex the coupling constant $g_{\pi NN^*}^2/4\pi = 3.4$ [Eq. (6)] and, rather arbitrarily, the same form factor as for the πNN vertex [15], $F_{\pi NN^*} = (\Lambda_\pi^2 - m_\pi^2)/(\Lambda_\pi^2 - q^2)$, where $\Lambda_\pi = 0.7$ GeV.

Neglecting first the width of the Roper resonance, the expression for the differential cross section of the $\gamma p \rightarrow \omega N^{*+}(1440)$ reaction reads

$$\begin{aligned} \frac{d\sigma}{dq^2}^{\gamma p \rightarrow \omega N^{*+}(1440)} &= \alpha \frac{g_{\pi\rho\omega}^2}{4\pi} \frac{g_{\pi NN^*}^2}{4\pi} \frac{\pi^2}{4g_\rho^2} \frac{(\hbar c)^2}{m_\omega^2} \frac{1}{E_\gamma^2} \frac{(M_{N^*}^0 - M_p)^2 - q^2}{4M_p^2} \\ &\quad \left[\frac{m_\omega^2 - q^2}{m_\pi^2 - q^2} \right]^2 \left[\frac{\Lambda_\pi^2 - m_\pi^2}{\Lambda_\pi^2 - q^2} \right]^2 \left[\frac{m_\rho^2 - m_\pi^2}{m_\rho^2 - q^2} \right]^2, \quad (18) \end{aligned}$$

where E_γ is the incident photon energy, q^2 the 4-momentum transfer and g_ρ is defined by the current-field identity [20]

$$\mathcal{J}_\mu^{em}(I=1) = \frac{em_\rho^2}{2g_\rho} \rho_\mu \quad (19)$$

and has the value $g_\rho^2 = 6.33$ [15].

The large width of the Roper resonance should however be included in the calculation of the $\gamma p \rightarrow \omega N^{*+}(1440)$ reaction near threshold. We estimate here the cross section in the $\pi^0 p$ decay channel, as the $\omega \pi^0 p$ final state of the $\gamma p \rightarrow \omega N^{*+}(1440)$ process could be measured for example at ELSA (with the Crystal Barrel) by detecting five photons in the final state [22]. Introducing the $N^{*+}(1440)$ propagator and decay vertex and denoting by κ the right-hand side of Eq. (18) divided by $[(M_{N^*}^0 - M_p)^2 - q^2]/4M_p^2$, we have

$$\frac{d\sigma}{dq^2} \gamma p \rightarrow \omega N^{*+}(1440) \rightarrow \omega \pi^0 p = \kappa \int_{m_{\pi^0} + M_p}^{M_{N^*}^{max}(E_\gamma, q^2)} dM_{N^*} \frac{(M_{N^*} - M_p)^2 - q^2}{4M_p^2} \frac{2\pi^{-1} M_{N^*} M_{N^*}^0 \Gamma_{N^{*+}(1440) \rightarrow \pi^0 p}(M_{N^*})}{(M_{N^*}^0)^2 - M_{N^*}^2 + M_{N^*}^0 \Gamma_{N^{*+}(1440)}^{tot}(M_{N^*})}, \quad (20)$$

in which $M_{N^*}^{max}(E_\gamma, q^2)$ is the maximum mass of the Roper resonance reachable for fixed incident photon energy E_γ and 4-momentum transfer q^2 . The energy-dependent widths of the $N^{*+}(1440)$ vanish for $M_{N^*} < m_{\pi^0} + M_p$ and are given, for $M_{N^*} > m_{\pi^0} + M_p$, by

$$\Gamma_{N^{*+}(1440) \rightarrow \pi^0 p}(M_{N^*}) = \Gamma_{N^{*+}(1440) \rightarrow \pi^0 p}(M_{N^*}^0) \frac{M_{N^*}^0}{M_{N^*}} \left[\frac{E(M_{N^*}) - M_N}{E(M_{N^*}^0) - M_N} \right] \frac{p[E(M_{N^*})]}{p[E(M_{N^*}^0)]}, \quad (21)$$

for the partial decay width of the $N^{*+}(1440)$ into the $\pi^0 p$ channel and

$$\Gamma_{N^{*+}(1440)}^{tot}(M_{N^*}) = \Gamma_{N^{*+}(1440)}^{tot}(M_{N^*}^0) \frac{M_{N^*}^0}{M_{N^*}} \left[\frac{E(M_{N^*}) - M_N}{E(M_{N^*}^0) - M_N} \right] \frac{p[E(M_{N^*})]}{p[E(M_{N^*}^0)]}, \quad (22)$$

for the total width, whose energy dependence is taken to be the same as for the partial width into the πN channel (which dominates the Roper resonance decay). $E(M_{N^*})$ is defined by Eq. (3). We take $\Gamma_{N^{*+}(1440) \rightarrow \pi^0 p}(M_{N^*}^0) = 76$ MeV and $\Gamma_{N^{*+}(1440)}^{tot}(M_{N^*}^0) = 350$ MeV, following the discussion of Section 2.1.

3.2 The $\gamma p \rightarrow \rho^0 N^{*+}(1440)$ reaction

In the case of the $\gamma p \rightarrow \rho^0 N^{*+}(1440)$ reaction, we calculate both the π - and σ -exchange contributions shown in Fig. 5. In view of the uncertainty in the $\sigma N N^{*+}(1440)$ coupling, the relative strength of both processes can but be settled by experimental data. We choose as before $E_\gamma = 2.5$ GeV.

The π -exchange contribution is computed with the same coupling constants and form factors as those used for the $\gamma p \rightarrow \omega N^{*+}(1440)$ reaction discussed in the previous subsection. The calculation of the σ -exchange contribution parallels that of Ref. [15]. The $\rho^0 \sigma \rho^0$ coupling is given by the Lagrangian,

$$\mathcal{L}_{\rho^0 \sigma \rho^0}^{int} = \frac{1}{2} \frac{g_{\sigma \rho \rho}}{m_\rho} \left[\partial^\alpha \rho^{0\beta} \partial_\alpha \rho_\beta^0 - \partial^\alpha \rho^{0\beta} \partial_\beta \rho_\alpha^0 \right] \sigma, \quad (23)$$

with a $\sigma \rho \rho$ form factor of the monopole form $(\Lambda_{\sigma \rho \rho}^2 - m_\sigma^2)/(\Lambda_{\sigma \rho \rho}^2 - q^2)$. The values of $g_{\sigma \rho \rho}$ and $\Lambda_{\sigma \rho \rho}$ are determined from a fit to $\gamma p \rightarrow \rho^0 p$ data to be $g_{\sigma \rho \rho}^2/4\pi=14.8$ and $\Lambda_{\sigma \rho \rho}=0.9$ GeV [15]. The σNN^* interaction Lagrangian is given in Eq. (7) and the value of the coupling constant in Eq. (14). The associated form factor is $(\Lambda_\sigma^2 - m_\sigma^2)/(\Lambda_\sigma^2 - q^2)$. We choose rather arbitrarily $\Lambda_\sigma=1$ GeV, as in the case of the σNN coupling [15]. We take $m_\sigma^0=500$ MeV.

The expression for the differential cross section of the $\gamma p \rightarrow \rho^0 N^{*+}(1440)$ reaction, analogous to Eq. (18) for the ω production, reads

$$\begin{aligned} \frac{d\sigma}{dq^2} \gamma p \rightarrow \rho^0 N^{*+}(1440) &= \alpha \frac{g_{\pi \rho \omega}^2}{4\pi} \frac{g_{\pi NN^*}^2}{4\pi} \frac{\pi^2}{4g_\omega^2} \frac{(\hbar c)^2}{m_\omega^2} \frac{1}{E_\gamma^2} \frac{(M_{N^*}^0 - M_p)^2 - q^2}{4M_p^2} \\ &\quad \left[\frac{m_\rho^2 - q^2}{m_\pi^2 - q^2} \right]^2 \left[\frac{\Lambda_\pi^2 - m_\pi^2}{\Lambda_\pi^2 - q^2} \right]^2 \left[\frac{m_\rho^2 - m_\pi^2}{m_\rho^2 - q^2} \right]^2 \\ &+ \alpha \frac{g_{\sigma \rho \rho}^2}{4\pi} \frac{g_{\sigma NN^*}^2}{4\pi} \frac{\pi^2}{4g_\rho^2} \frac{(\hbar c)^2}{m_\rho^2} \frac{1}{E_\gamma^2} \frac{(M_{N^*}^0 + M_p)^2 - q^2}{4M_p^2} \\ &\quad \left[\frac{m_\rho^2 - q^2}{m_\sigma^2 - q^2} \right]^2 \left[\frac{\Lambda_\sigma^2 - m_\sigma^2}{\Lambda_\sigma^2 - q^2} \right]^2 \left[\frac{\Lambda_{\sigma \rho \rho}^2 - m_\sigma^2}{\Lambda_{\sigma \rho \rho}^2 - q^2} \right]^2, \quad (24) \end{aligned}$$

where g_ω is defined by the current-field identity [20]

$$\mathcal{J}_\mu^{em}(I=0) = \frac{em_\omega^2}{2g_\omega} \omega_\mu \quad (25)$$

and has the value $g_\omega^2 = 72.71$ [15].

In Eq. (24), the Roper resonance has no width. We include it and calculate the cross section for the $\gamma p \rightarrow \rho^0 N^{*+}(1440)$ reaction in the $\rho^0 \pi^+ n$ decay channel. The ρ^0 will indeed decay into a $\pi^+ \pi^-$ pair. It is therefore natural to study this process with three charged pions in the final state. Denoting by κ_1 and κ_2 the first and second terms of the right-hand side of Eq. (24) divided by $[(M_{N^*}^0 - M_p)^2 - q^2]/4M_p^2$ and $[(M_{N^*}^0 + M_p)^2 - q^2]/4M_p^2$ respectively, we have, in complete analogy with Eq. (20),

$$\begin{aligned} \frac{d\sigma}{dq^2} \gamma p \rightarrow \rho^0 N^{*+}(1440) \rightarrow \rho^0 \pi^+ n &= \int_{m_{\pi^+} + M_n}^{M_{N^*}^{max}(E_\gamma, q^2)} dM_{N^*} \left(\kappa_1 \frac{(M_{N^*} - M_p)^2 - q^2}{4M_p^2} \right. \\ &\left. + \kappa_2 \frac{(M_{N^*} + M_p)^2 - q^2}{4M_p^2} \right) \frac{2\pi^{-1} M_{N^*} M_{N^*}^0 \Gamma_{N^{*+}(1440) \rightarrow \pi^+ n}(M_{N^*})}{(M_{N^*}^0)^2 - M_{N^*}^2)^2 + M_{N^*}^0 \Gamma_{N^{*+}(1440)}^{2tot}(M_{N^*})}. \end{aligned} \quad (26)$$

The energy dependence of the partial and total widths is the same as in Eqs. (21) and (22). We remark however that $\Gamma_{N^{*+}(1440) \rightarrow \pi^+ n}(M_{N^*}^0) = 152$ MeV, because of the isospin factor.

4 Numerical results

4.1 The $\gamma p \rightarrow \omega N^{*+}(1440)$ reaction

The differential cross section for the $\gamma p \rightarrow \omega N^{*+}(1440)$ reaction at $E_\gamma=2.5$ GeV given by Eq. (18), i.e. neglecting the width of the Roper resonance, is shown in Fig. 6. Eventhough we have plotted the differential cross section in this figure (and in the subsequent ones) until $q^2=-0.7$ GeV², we do not expect our model to be valid much beyond $q^2=-0.5$ GeV². This limit is set by the cut-off in the $\pi N N^*$ form factor, $\Lambda_\pi=0.7$ GeV. In the zero-width approximation for the $N^*(1440)$, the lowest value of q^2 (corresponding to $\theta = 0^\circ$) is -0.36 GeV².

Taking into account the width of the Roper resonance, we show in Fig. 7 the differential cross section for the $\gamma p \rightarrow \omega N^{*+}(1440)$ reaction assuming that the $N^{*+}(1440)$ decays subsequently into the $\pi^0 p$ channel ($E_\gamma=2.5$ GeV). The curve represents the expression given in Eq. (20), completed by the energy-dependent widths (21) and (22).

Much smaller values of $-q^2$ are reachable when the low-energy tail of the Roper resonance is explicitly included. At $q^2=-0.36$ GeV², the differential cross section for the $\gamma p \rightarrow \omega N^{*+}(1440) \rightarrow \omega \pi^0 p$ reaction is about 20 times smaller than the differential cross section for $\gamma p \rightarrow \omega N^{*+}(1440)$ in the zero-width approximation. This number can be easily understood. The partial decay width of the $N^{*+}(1440)$ into the $\pi^0 p$ channel is roughly 20% and the interval of M_{N^*} involved in the integral of Eq. (20) reduces the strength for the excitation of the Roper resonance by a factor of about 4 compared to the situation where all the strength is concentrated at $M_{N^*}^0=1.44$ GeV.

If our simple π -exchange model of the $\gamma p \rightarrow \omega N^{*+}(1440)$ reaction near threshold makes sense, the measurement of the cross section displayed in Fig. 7 would bring strong constraints on the $\pi N N^*$ vertex. It is interesting that a new mea-

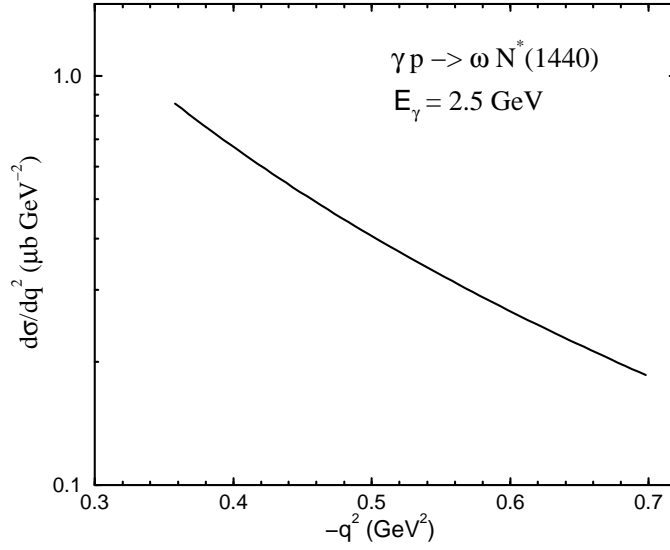


Fig. 6. Differential cross section for the $\gamma p \rightarrow \omega N^{*+}(1440)$ reaction at $E_\gamma=2.5$ GeV in the one-pion exchange model and in the zero-width approximation for the $N^*(1440)$. The parameters are given in subsection 3.1.

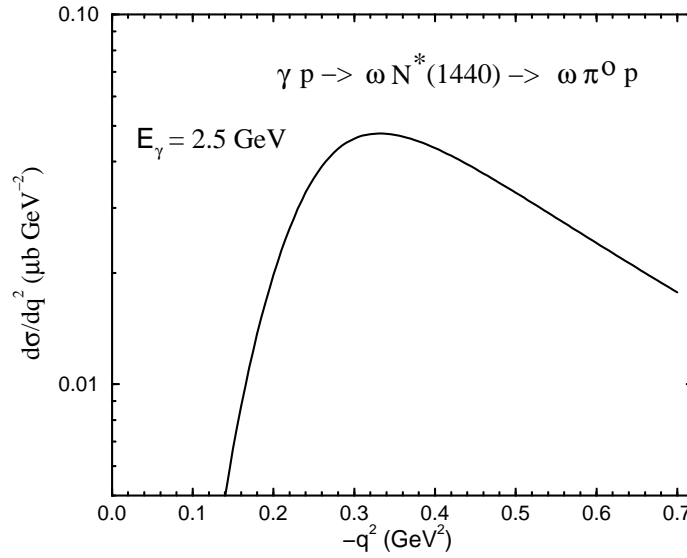


Fig. 7. Differential cross section for the $\gamma p \rightarrow \omega N^{*+}(1440) \rightarrow \omega \pi^0 p$ reaction at $E_\gamma=2.5$ GeV in the one-pion exchange model. The parameters are given in subsection 3.1.

surement of the $\omega \rightarrow \pi^0 e^+ e^-$ form factor, planned in the near future by the HADES Collaboration at GSI [23], will provide a better understanding of the $\omega\rho\pi$ vertex and additional control on the left-hand graph of Fig. 4.

4.2 The $\gamma p \rightarrow \rho^0 N^{*+}(1440)$ reaction

The differential cross section for the $\gamma p \rightarrow \rho^0 N^{*+}(1440)$ reaction at $E_\gamma=2.5$ GeV given by Eq. (24), in the zero-width approximation for the Roper resonance, is shown in Fig. 8. We have plotted separately the contributions from the π - and σ -exchanges.

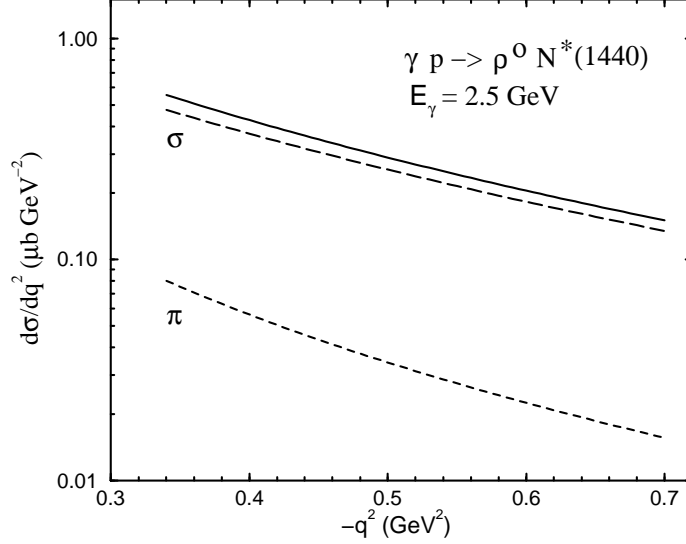


Fig. 8. Differential cross section for the $\gamma p \rightarrow \rho^0 N^{*+}(1440)$ reaction at $E_\gamma=2.5$ GeV in the one-meson exchange model and in the zero-width approximation for the $N^*(1440)$. The contributions of the π - and σ -exchanges are indicated by long-dashed and short-dashed lines respectively. The parameters are given in subsection 3.2.

The σ -exchange contribution appears largely dominant. We recall however that the σNN^* coupling constant has a very substantial error bar. We took $g_{\sigma NN^*}^2/4\pi=0.34$, according to Eq. (14). As discussed in Section 2.2, the uncertainty in this quantity is typically of a factor 5. If our $(\pi+\sigma)$ -exchange model of the $\gamma p \rightarrow \rho^0 N^{*+}(1440)$ reaction near threshold is a proper description of this process, the measurement of the corresponding cross section would place strong constraints on $g_{\sigma NN^*}$.

Releasing the zero-width approximation for the $N^*(1440)$ and looking at its $\pi^+ n$ decay channel [Eq. (26)], yield the curve displayed in Fig. 9.

At $q^2=-0.36$ GeV², the differential cross section for the $\gamma p \rightarrow \rho^0 N^{*+}(1440) \rightarrow \rho^0 \pi^+ n$ reaction is only 10 times smaller than the differential cross section for $\gamma p \rightarrow \rho^0 N^{*+}(1440)$ in the zero-width approximation because the $N^*(1440) \rightarrow \pi^+ n$ decay width is twice larger than the $N^*(1440) \rightarrow \pi^0 p$ decay width. For simplicity, we have not included explicitly the ρ^0 -meson width. Near threshold,

it would reduce further the differential cross section by a factor of about 2.

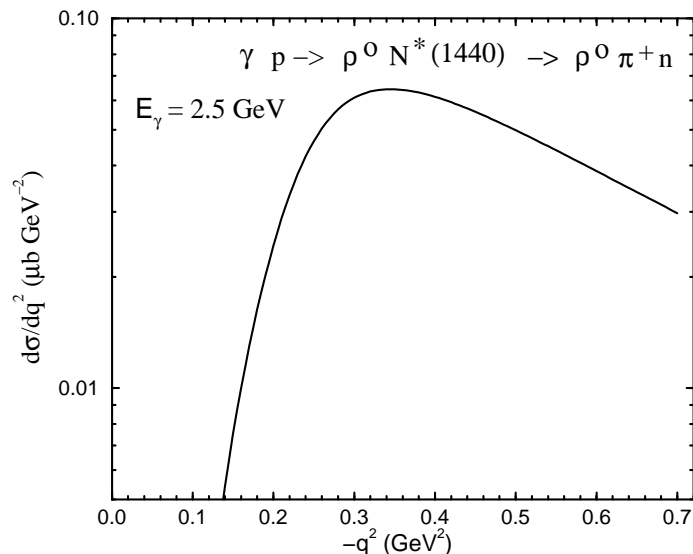


Fig. 9. Differential cross section for the $\gamma p \rightarrow \rho^0 N^{*+}(1440) \rightarrow \rho^0 \pi^+ n$ reaction at $E_\gamma = 2.5$ GeV in the $(\pi + \sigma)$ -exchange model. The parameters are given in subsection 3.2.

A very interesting experimental possibility to disentangle π - and σ -exchanges in the $\gamma p \rightarrow \rho^0 N^{*+}(1440)$ reaction would be to study this process with linearly polarized photons. Such experiment would indeed offer the possibility to separate natural and unnatural parity exchanges in the t-channel [24].

5 Conclusion

We propose a simple, and probably the first, model to describe the associate photoproduction of vector mesons ($\rho^0(770)$ and $\omega(782)$) and $N^{*+}(1440)$ resonances from proton targets. The domain of applicability of this model, involving t-channel π - and σ -exchanges, is restricted to photon energies leading to ρ^0 and ω production close to threshold ($E_\gamma < 3$ GeV) and to low momentum transfers ($|q^2| \leq 0.5\text{--}0.6$ GeV²).

At $E_\gamma = 2.5$ GeV, the total cross section for these processes is predicted to be typically of the order of 50 nb, with sizeable theoretical uncertainty.

The $\gamma p \rightarrow \omega N^{*+}(1440)$ amplitude is given entirely by pion-exchange, while the $\gamma p \rightarrow \rho^0 N^{*+}(1440)$ amplitude appears largely dominated by σ -exchange. We suggest that a measurement of the latter process, particularly with linearly polarized photons, would provide very significant constraints on the σNN^*

coupling while data on the former reaction would pin down the πNN^* coupling.

Contributions other than the above processes to a given final state should however be estimated to assess the relevance of the proposed measurements.

In general, it seems that the most favourable conditions to observe the $\gamma p \rightarrow \omega N^{*+}(1440)$ and $\gamma p \rightarrow \rho^0 N^{*+}(1440)$ reactions would be photon incident energies and values of the momentum transfer q^2 chosen so as to excite the low-energy tail of the Roper resonance. For $E_\gamma = 2.5$ GeV, this implies values of $|q^2|$ less than about 0.4 GeV². Such kinematics would suppress overlaps with the $N^{*+}(1520)$ and the $N^{*+}(1535)$ resonances which decay largely into the πN channel. In this regime, the main competing processes in our t-channel model would be $\gamma p \rightarrow \omega \Delta^+(1232)$ and the $\gamma p \rightarrow \rho^0 \Delta^+(1232)$ reactions. The corresponding amplitudes can be quite reliably calculated as the coupling of the $\Delta(1232)$ to the πN channel has been very extensively studied. The $\Delta(1232)$ excitation is suppressed in processes where the σ -exchange is dominant. One should note also that in experiments where the $N^{*+}(1440)$ resonance could be identified by its decay into the $\pi\pi N$ channel, rather than in the πN channel as proposed in this paper, the $\Delta(1232)$ amplitude mentioned above would not contribute. It is important to keep in mind however that the role of s-channel resonances in the 2.5 GeV range is at present very poorly known.

6 Acknowledgements

The author is very much indebted to Berthold Schoch who suggested the work presented in this paper in relation with an experimental project at the Bonn ELSA Facility. She thanks Nathan Isgur for an extremely useful remark. She acknowledges very helpful discussions with Marcel Morlet and Dan-Olof Riska.

References

- [1] Review of Particle Physics, Eur. Phys. J. C 3, (1998) 1.
- [2] S. A. Coon, M. T. Peña and D. O. Riska, Phys. Rev. C 52 (1995) 2925.
- [3] H. Kamada and W. Glöckle, Nucl. Phys. A 560 (1993) 541.
- [4] M. T. Peña, D. O. Riska and A. Stadler, Phys. Rev. C 60 (1999) 045201.
- [5] T.-S. H. Lee and D. O. Riska, Phys. Rev. Lett. 70 (1993) 2237.
- [6] V. Metag, Nucl. Phys. A 553 (1993) 283c.
- [7] W. Ehehalt et al., Phys. Rev. C 47 (1993) 2467.
- [8] S. Teis et al., Z. Phys. A 356 (1997) 421.
- [9] B.-A. Li, C. M. Ko and G. Q. Li, Phys. Rev. C 50 (1994) 2675.
- [10] S. Huber and J. Aichelin, Nucl. Phys. A 573 (1994) 587.
- [11] G. Mao et al., Phys. Rev. C 57 (1998) 1938.
- [12] M. Eskef et al., Eur. Phys. J. A 3 (1998) 335.
- [13] J. A. Gómez Tejedor and E. Oset, Nucl. Phys. A 571 (1994) 667.
- [14] H. Garcilazo and E. Moya de Guerra, Nucl. Phys. A 562 (1993) 521.
- [15] B. Friman and M. Soyeur, Nucl. Phys. A 600 (1996) 477.
- [16] H.P. Morsch et al, Phys. Rev. Lett. 69 (1992) 1336.
- [17] S. Hirenzaki, P. Fernández de Córdoba and E. Oset, Phys. Rev. C53 (1996) 277.
- [18] S. Hirenzaki et al, in preparation.
- [19] Aachen-Berlin-Bonn-Hamburg-Heidelberg-München Collaboration, Phys. Rev. 175 (1968) 1669.
- [20] N.M. Kroll, T.D. Lee and B. Zumino, Phys. Rev. 157 (1967) 1376.
- [21] M. Chemtob in Mesons and Nuclei (Eds. M. Rho and D. Wilkinson, North-Holland, 1979), Vol. II, p 495.
- [22] B. Schoch, private communication.
- [23] HADES Proposal, GSI Internal Report and private communication.
- [24] J. Ballam et al, Phys. Rev. 7 (1973) 3150.